PLOS ONE

RESEARCH ARTICLE

On the mechanism of *Candida tropicalis* biofilm reduction by the combined action of naturally-occurring anthraquinones and blue light

Juliana Marioni[1☯], Roger Bresolí-Obach[2☯], Montserrat Agut[2], Laura R. Comini[1], José L. Cabrera[1], María G. Paraje[3], Santi Nonell[2]*, Susana C. Núñez Montoya[1]*

1 IMBIV, CONICET and Departamento de Ciencias Farmacéuticas, Facultad de Ciencias Químicas, Universidad Nacional Córdoba, Córdoba, Argentina, **2** Institut Químic de Sarrià, Universitat Ramon Llull, Barcelona, Spain, **3** IMBIV, CONICET and Cátedra de Microbiología, Facultad de Ciencias Exactas Físicas y Naturales, Universidad Nacional de Córdoba, Córdoba, Argentina

☯ These authors contributed equally to this work.
* santi.nonell@iqs.url.edu (SN); sununez@fcq.unc.edu.ar (SCNM)

Citation: Marioni J, Bresolí-Obach R, Agut M, Comini LR, Cabrera JL, Paraje MG, et al. (2017) On the mechanism of *Candida tropicalis* biofilm reduction by the combined action of naturally-occurring anthraquinones and blue light. PLoS ONE 12(7): e0181517. https://doi.org/10.1371/journal.pone.0181517

Editor: Michael Hamblin, Massachusetts General Hospital, UNITED STATES

Received: August 15, 2016

Accepted: July 3, 2017

Published: July 19, 2017

Data Availability Statement: All relevant data are within the paper and its Supporting Information files.

Funding: This study was funded by Fondo para investigación Científica y Tecnológica. Plan Argentina Innovadora 2020, tipo A, PICT 2014 n° 2204, http://www.agencia.mincyt.gob.ar/frontend/agencia/fondo/foncyt JLC; Consejo Nacional de Investigaciones Científicas y Técnicas, PIP 2013-2015, s/ res. GI 4316/2013, http://www.conicet.

Abstract

The photoprocesses involved in the photo-induced *Candida tropicalis* biofilm reduction by two natural anthraquinones (AQs), rubiadin (**1**) and rubiadin-1-methyl ether (**2**), were examined. Production of singlet oxygen ($^1O_2$) and of superoxide radical anion ($O_2^{\bullet-}$) was studied. Although it was not possible to detect the triplet state absorption of any AQs in biofilms, observation of $^1O_2$ phosphorescence incubated with deuterated Phosphate Buffer Solution, indicated that this species is actually formed in biofilms. **2** was accumulated in the biofilm to a greater extent than **1** and produced measurable amounts of $O_2^{\bullet-}$ after 3h incubation in biofilms. The effect of reactive oxygen species scavengers on the photo-induced biofilm reduction showed that Tiron (a specific $O_2^{\bullet-}$ scavenger) is most effective than sodium azide (a specific $^1O_2$ quencher). This suggests that $O_2^{\bullet-}$ formed by electron transfer quenching of the AQs excited states, is the main photosensitizing mechanism involved in the photo-induced antibiofilm activity, whereas $^1O_2$ participation seems of lesser importance.

Introduction

Antimicrobial photodynamic therapy is an emerging approach for treating infections in which activation of a photosensitising substance by light in the presence of oxygen increases the levels of reactive oxygen species (ROS) and induces oxidative stress in the pathogenic microorganisms [1,2]. Thus, the scrutiny of new photosensitisers (PSs), particularly of natural origin, is a research area currently under intensive development [2,3]. Our research team is interested in investigating the potential use in antimicrobial photodynamic therapy of a group of natural 9,10-anthraquinone aglycones (AQs) with photosensitizing properties.

Candida species are the yeasts most commonly associated with hospital-acquired infections, which cause both superficial and systemic diseases [1,4,5]. The well-known resistance of

gov.ar/ JLC; Secretaria de Ciencia y Técnica, Universidad Nacional de Córdoba, Categoría A, s/ res. n° 203/14, http://www.unc.edu.ar/investigacion/financiamiento/subsidios-e-incentivos SCNM; Ministerio de Economía y Competitividad, CTQ2013-48767-C3-1-R, http://www.mineco.gob.es/portal/site/mineco/idi SN.

Competing interests: The authors have declared that no competing interests exist.

Candida spp. to conventional antifungal therapies is a complex multifactorial phenomenon, caused in part by the development of biofilms [1,4–7]. Although *C. albicans* is the main etiologic agent of hospital-acquired infections, *C. tropicalis* has been noted as one of the most frequently isolated pathogenic yeasts in nosocomial candidiasis in recent years, especially in Latin America [8,9]. *C. tropicalis* biofilms is usually related with patients with neutropenia and malignancy, and even associated with higher mortality than other *Candida* no *albicans* spp. [4,5,7–9].

Rubiadin (**1**) and rubiadin-1-methyl ether (**2**) (Fig 1) are two AQs isolated from the phototoxic plant *Heterophyllaea pustulata* Hook f. (*Rubiaceae*) [10,11]. This plant species grows in the Andean region of northwestern Argentina and Bolivia, where is popularly known as "cegadera", "ciegadera" o "saruera" [12]. Photoactivation of a *H. pustulata* extract containing both AQs produced a reduction of 39.3 ± 3.5% in the growth of *C. tropicalis* biofilms. The concentration necessary to inhibit the biofilm (Biofilm Inhibitory Concentration) [13] was 0.2 mg/mL. Meanwhile, both purified AQs, **1** and **2**, showed greater antibiofilm effect than the photoactive extract under irradiation, which was mediated by a strong redox imbalance. Rubiadin was more active than its methylated derivative, since lower concentration was required to achieve similar values of reduction (1.96 μg/mL for **1** and 15.6 μg/mL for **2**, Table 1 and 2 in S1 File) [14].

We have previously established that the two AQs possess interesting photophysical and photosensitising properties [15, 16]. Both compounds absorb in the UV and blue regions of the spectrum (i.e. maximum absorbance at 411 and 360 nm, respectively) and are poorly fluorescent ($\Phi_F \approx 10^{-2}$) in chloroform ($CHCl_3$).

In this work, we set out to identify the reactive intermediates involved in the photo-induced *C. tropicalis* biofilm reduction by two natural AQs: rubiadin and rubiadin-1-methyl ether.

Materials and methods

Chemicals

The following chemicals were used as received: Crystal Violet (CV, Anedra Tigre, Argentina); Fetal Bovine Serum (Greiner Bio-One, Frickenhausen, Germany); Sabouraud Dextrose Broth (SDB, Difco, Detroit, MI); Sabouraud dextrose agar (Difco, Detroit, MI), Phosphate Buffer Solution (PBS); dimethyl sulfoxide (DMSO, Merck Darmstadt, Germany); Calcofluor-White (Sigma-Aldrich Co, St Louis, MO, USA); MeOH (HPLC grade, Merck, Germany); Nitro Blue Tetrazolium (NBT, Sigma-Aldrich Co, St Louis, MO, USA); Methionine (Sigma-Aldrich);

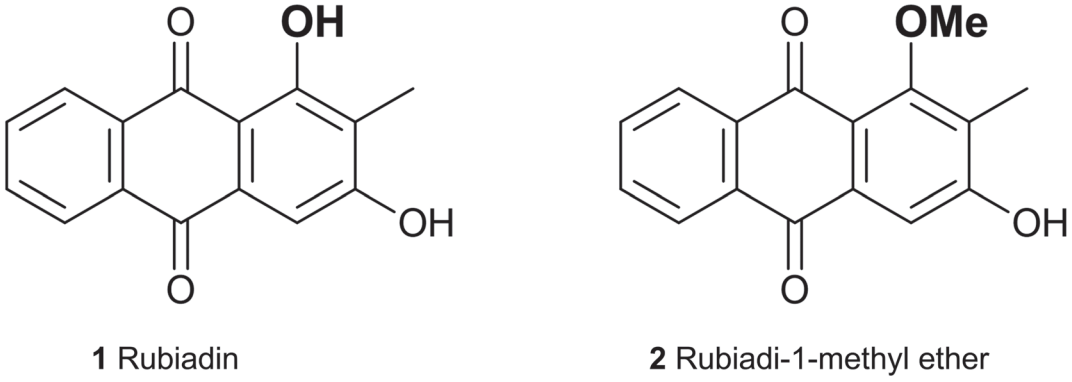

Fig 1. Chemical structure of rubiadin (1) and rubiadin-1-methyl ether (2).

https://doi.org/10.1371/journal.pone.0181517.g001

Riboflavin (Sigma-Aldrich Co, St Louis, MO, USA), Tiron (Sigma-Aldrich); Sodium azide (Sigma-Aldrich).

Deuterium oxide (99.9%) was purchased from Solvents Documentation Synthesis (Peypin, France). Deuterated PBS (D-PBS) was prepared by dissolving PBS powder in deuterium oxide.

1 and **2** were purified from benzene extracts of *H. pustulata* using a methodology described previously [10,11]. They were unequivocally identified by their spectroscopic/spectrometric data (^{1}H NMR, ^{13}C NMR, IR, UV–Vis, MS) [10]. The purity was 93.6% ± 0.1% for **1** and 93.8 ± 0.1% for **2**, as established by HPLC analysis [13] (Fig 2 in S1 File).

Yeast strain conditions

Stock solution of *C. tropicalis* NCPF 3111 (National Collection of Pathogenic Fungi, Bristol, UK, strain N° 2), suspended in SDB with 10% glycerol (cryoprotectant), was kept at −80°C. In order to ensure purity and viability of yeasts before its use, they were plated in Sabouraud dextrose agar and then were incubated overnight in Falcon tubes at 37°C with SDB [14,17].

Photosensitiser solutions

Each stock AQs solution was prepared in SDB with 1% DMSO. Then, a dilution with the culture medium was performed to obtain a final concentration of 56 μM for each AQ, and these solutions were stored in the dark at 4°C. All solutions were prepared and handled under light-restricted conditions.

DMSO was used to solubilize drugs in aqueous solutions, as this is a common *in vitro* practice to deliver hydrophobic drugs to cells. DMSO is a good scavenger for hydroxyl radicals, but has no effect on $^{1}O_2$ at the concentration used in our studies [18]. In addition, 1% DMSO has no effect either on the rate of $O_2^{\bullet-}$ production by neutrophils [19].

Light sources

An actinic Phillips 20 W lamp (380–480 nm, emission maximum at 420 nm, 0.65 mW cm^{-2}) was used in photo-induced antibiofilm studies, which was placed 20 cm above the samples inside a black box [13,14].

In vitro photo-induced biofilm reduction assays

Biofilm formation was achieved following the previously published procedure [13,14,20], which is an adaptation from the method of O'Toole & Kolter (1998) [21] using flat-bottomed 96-well microplates (Greiner Bio-One, Germany). In this assay, we used the *C. tropicalis* NCPF 3111 strain previously classified as a strong biofilm producer [13,22]. A strain suspension (1×10^7 cells/mL) in SDB was inoculated in pre-treated microplates with 50% (v/v) Fetal Bovine Serum [19], and then were incubated 90 min at 37°C. After removing the non-adhered cells and add fresh culture medium, the incubation of microplates was resumed at the same temperature during 48 h without stirring to obtain a dense biofilm [13]. Formation of the biofilm was demonstrated by confocal laser scanning microscopy (CLSM, Fig 2) [13,20,23]. Each AQs solution (56 μM) was added in triplicate onto the dense biofilm, pre-washed with sterile PBS. Control wells, containing only SDB and 1% DMSO at pH = 6.5, were included in triplicate. Two replicates of the microplates were prepared, whereas one was kept in the dark, the other was irradiated for 15 min [13,14]. Subsequently, both microplates were incubated 48 h at 37°C. After incubation, supernatant was separated to assess the production of $O_2^{\bullet-}$ and SOD activity [13,14]. The total biomass of the biofilm formed was quantified by staining with a CV solution (1% w/v).To this end, the excess dye was first removed by washing with PBS and CV

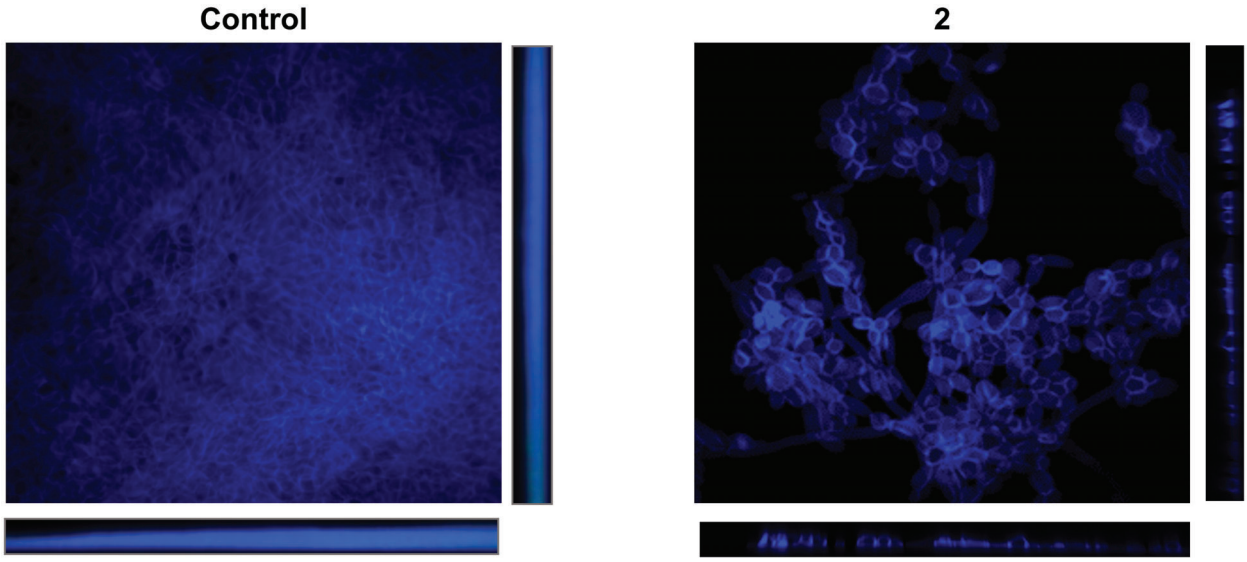

Fig 2. CSLM images showing the effect of rubiadin 1-methyl ether and blue light on *C. tropicalis* NCPF 3111 biofilms. (A) Positive control, (B) rubiadin 1-methyl ether (56 μM). Blue channel shows Calcofluor white dying sessile cells walls. Magnification 60X and scale bar is 10 μm.

https://doi.org/10.1371/journal.pone.0181517.g002

was extracted from the biomass with an ethanol/acetone (70:30) solution. Optical density (OD) was measured at 595 nm by using a microplate reader (Tecan Sunrise Model, TECAN, AUS). The average OD of all tested wells (n = 3) was obtained by subtracting the average OD from control wells (ODc). The biomass of the formed biofilm was expressed in biofilm biomass units (BBU), defined as 0.1 OD_{595} corresponding to 1 BBU [13,20].

AQ accumulation assay in biofilms

Dense biofilms formed as described above in 24-well microplates, were exposed to 56 μM of **1** and **2** in SBD, respectively in duplicate, during 0.5, 1, 3 and 6 h. Control samples (in duplicate) were processed without AQ under the same working conditions. After incubation at 37˚C, biofilms of each microwell (treated and controls) were collected separately by scraping. Each pellet obtained by centrifugation at 5000 rpm for 25 min, was suspended in $CHCl_3$ (1 mL) and was exposed alternatively to cold and heat, using liquid air and a thermostatic water-bath at 70 ˚C. This procedure was repeated three times in order to break down the biofilm structures. $CHCl_3$ was then used to disrupt the phospholipid bilayer of the cell membranes and extract the AQs from the biofilms [24], since their high logP values (2.26 for **1** and 2.83 for **2**) [25] indicate their preferential solubility in nonpolar solvents and accumulation in lipophilic compartments. The supernatant was evaporated to dryness and was dissolved in methanol for subsequent analysis by HPLC, following the procedure described before [13]. Once the scraping was finished, the microplate was stained with CV to verify that all biofilms were removed.

Spectroscopic measurements

Ground-state absorption spectra were recorded using a Varian Cary 6000i spectrophotometer (Varian Inc., Palo Alto, CA). Fluorescence emission spectra were recorded in a Spex Fluoromax-4 spectrofluorometer (Horiba Jobin-Yvon, Edison, NJ). Time resolved fluorescence decays were recorded with a time-correlated single photon counting system (Fluotime 200, PicoQuant GmbH, Berlin, Germany) equipped with a red-sensitive photomultiplier. The

fluorescence was excited at 375 nm by means of a pulsed laser diode working at 10 MHz repetition rate, and was observed at 420 nm keeping the counting frequency below 1%. Fluorescence decays were analysed using the PicoQuant FluoFit 4.5 data analysis software (PicoQuant, Germany) [26].

$^1O_2$ phosphorescence at 1275 nm was detected by means of a customized PicoQuant Fluotime 200 system using a diode-pumped pulsed Nd:YAG laser (FTSS355-Q, Crystal Laser, Berlin, Germany) working at 10 kHz repetition rate at 355 nm (6 mW, 0.6 μJ per pulse) for excitation. A 1064 nm rugate notch and a Schott KG5 filter (Edmund Optics, UK) were placed at the exit port of the laser to remove any residual component of its fundamental emission in the near-IR region. The emitted luminescence was filtered by using a cold mirror (CVI Melles Griot, USA) and an interference filter at 1273 ± 86 nm (Interferenzoptik Elektronik GmbH, Germany) and focused onto a near-IR sensitive photomultiplier tube assembly (H9170-45, Hamamatsu Photonics Hamamatsu City, Japan). Photon counting was achieved with a NanoHarp 250 multichannel scaler (PicoQuant, Germany). The time-resolved emission signals were likewise analyzed using the FluoFit 4.5 software to extract lifetime values [26]. $^1O_2$ production quantum yields (Φ_Δ) were determined by comparing the intensity of the signals to that of a standard measured under matched conditions [26]. Phenalenone, for which Φ_Δ = 0.95–1.0 in many solvents was used as standard [27,28].

Transient absorption experiments were carried out using a home-built nanosecond laser flash photolysis apparatus described elsewhere [27,28]. The excitation wavelength was 355 nm and the transient absorption was recorded at the appropriate wavelengths for monitoring the triplet state (^{3}AQ, 675 nm), the ketyl radical (AQ$^\bullet$, 450 nm) or the radical anion (AQ$^{\bullet-}$, 550 nm) of the rubiadins [29].

Dense biofilms were developed on a square glass plate (1 x 1 cm) in a 24-well microplate and the AQs (56 μM) were added as described above. After the incubation period, the supernatants were removed, the biofilms were washed twice with sterile PBS and the glass plates were introduced vertically in the spectroscopic cuvettes at 45 degrees relative to the excitation light beam. Then the appropriate aqueous buffer (PBS or deuterated PBS) was carefully added to fill the cuvette. Controls containing sessile cells of *C. tropicalis* in D-PBS were performed. In agreement with the report by Berry *et al.* [30], D-PBS had no effect on the biofilm biomass compared to PBS. Spectroscopic measurements were carried out without stirring to prevent mechanically disturbing the biofilms.

Effect of quenchers on the photo-induced biofilm reduction

Insight on the photo-induced biofilm reduction mechanism was gained by studying the effect of the ROS quenchers Tiron (for $O_2^{\bullet-}$) and sodium azide (for $^1O_2$) on a 48h-biofilm [31,32]. AQs (56 μM) and quenchers (500 mM) were added to biofilms at the same time, and the assay was performed in the dark and under irradiation using the conditions mentioned above. After 48 h incubation at 37˚C, the supernatant was removed in order to measure the $O_2^{\bullet-}$ production and the SOD activity. Biofilm formation was determined by CV, where BBU was calculated from OD measurements at 595 nm [13,14].

Production of $O_2^{\bullet-}$ was evaluated by reduction of NBT (1 mg/mL) which converts in an insoluble precipitate (Blue diformazan) by action of this ROS, so that the formed blue diformazan is proportional to the generated $O_2^{\bullet-}$ in biofilms, and was measured spectrophotometrically at 540 nm. Results were expressed as OD_{540nm}/BBU ($O_2^{\bullet-}$/BBU) [13,14].

Likewise, SOD activation was determined from the inhibition of NBT reduction by supernatant. $O_2^{\bullet-}$ was generated by photoexcitation of riboflavin in the presence of oxygen and of the electron donor methionine. The results were expressed as SOD activation (%)/BBU [13,14].

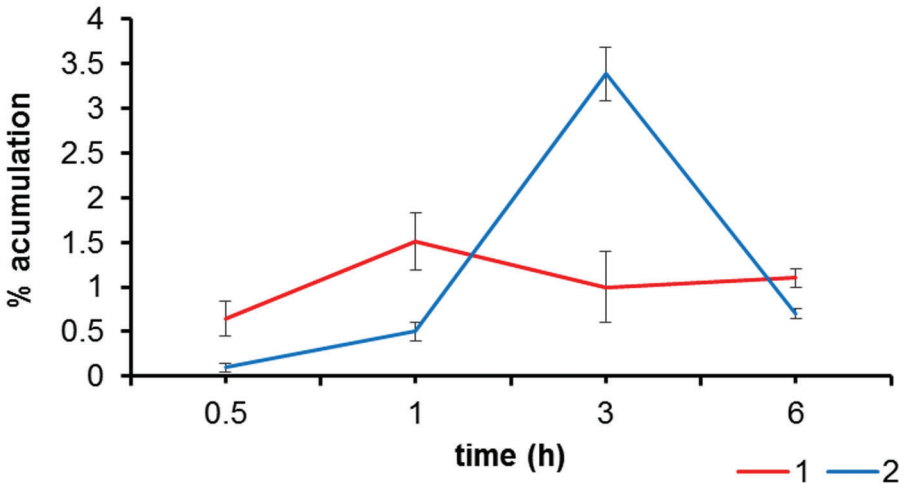

Fig 3. AQs accumulation in *C. tropicalis* biofilms by HPLC method.

https://doi.org/10.1371/journal.pone.0181517.g003

Statistical analysis

All assays were evaluated in triplicate and in 3 independent experiments. Results of all experiments were expressed as means values with standard deviations. Data were statistically analysed by using the Student-Newman-Keuls test for multiple comparisons and the post hoc Tukey's test. A p-value < 0.05 was considered statistically significant.

Results

In vitro fungal biofilm reduction

AQ **2** accumulates in the biofilms to a substantially greater extent than **1**, (3.4 ± 0.3% *vs* 1.1 ± 0.4%, respectively), relative to the AQs initial concentration and after 3h incubation (Fig 3). When kept in the dark, neither **1** nor **2** were active against *C. tropicalis* NCFP biofilms at the concentration tested (56 μM) (Table 1). On the other hand, exposure to light reduced the BBU by 3.2 and 2.6-fold, respectively ($p>0.05$ when **1** is compared with **2**). It should be noted that light alone did not show any inhibitory effect on biofilm growth. Likewise, DMSO had no effect either.

Absorption and fluorescence spectra

The absorption spectra of **1** and **2** in $CHCl_3$, PBS, planktonic yeast and biofilms are shown in Fig 4. The spectra in PBS and planktonic yeast were similar, with broader, red-shifted bands

Table 1. Mass of the biofilms (in BBU units) exposed to 56 μM rubiadin (1) or rubiadin 1-methyl ether (2) in the dark and under irradiation.

AQ	DARK	IRRADIATION
1	54 ± 3	18 ± 4*
2	50 ± 6	23 ± 8
Control**	57 ± 7	59 ± 5

p*>0.05 when **1 is compared with **2**

***No AQ added

https://doi.org/10.1371/journal.pone.0181517.t001

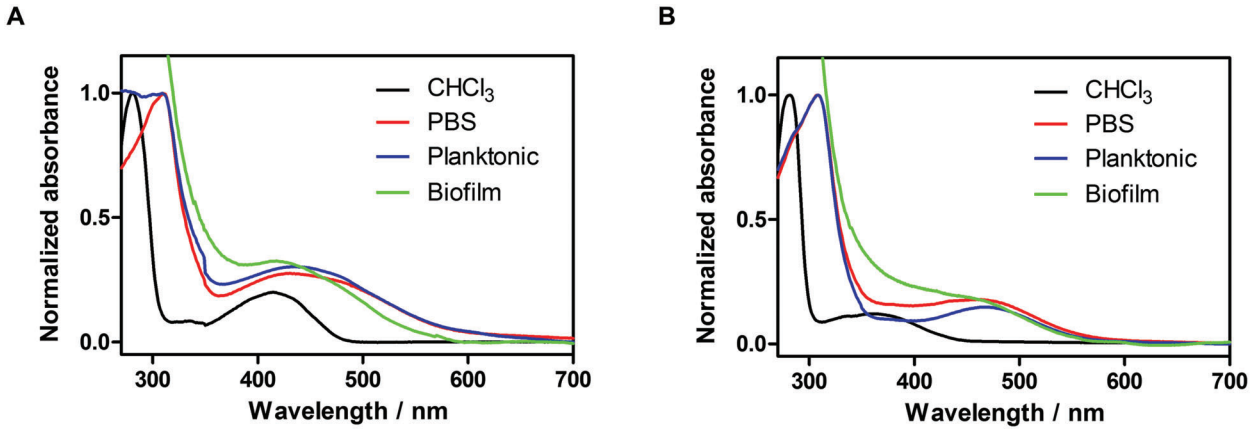

Fig 4. Absorption spectra of rubiadin (A) and rubiadin 1-methyl ether (B) (56 μM) in $CHCl_3$, PBS, planktonic yeast and biofilms of *C. tropicalis*.

https://doi.org/10.1371/journal.pone.0181517.g004

relative to $CHCl_3$ solutions. The red- shift is more pronounced for **2**. The spectra in biofilms showed a behaviour intermediate between $CHCl_3$ and PBS.

Although the fluorescence was very weak, it was possible to determine the lifetime of the singlet excited states, which was 0.9 ns in $CHCl_3$ and 0.60 ns in PBS for **1**. The corresponding values for **2** were 1.4 ns and 0.8 ns, respectively.

Transient absorption experiments

Formation of the triplet state, the ketyl radical and the radical anion of the AQs, ^{3}AQ and $AQ^{\bullet-}$ respectively, was studied by transient absorption spectroscopy in $CHCl_3$, PBS, planktonic yeast and biofilms. The corresponding wavelengths were 675 nm (^{3}AQ,), 450 nm ($AQ^{\bullet}$) and 550 nm ($AQ^{\bullet-}$). It was not possible to detect $AQ^{\bullet}$ or $AQ^{\bullet-}$ for **1** in any of the above systems, whereas large $AQ^{\bullet-}$ signals could be observed for **2** in $CHCl_3$ solutions (Fig 5). In argon-saturated $CHCl_3$ the transient rose with lifetime 4 μs and lived 450 μs, whereas in air-saturated solutions the rise was much faster and the lifetime was decreased to 150 μs. This indicates that $AQ^{\bullet-}$ is formed from ^{3}AQ and that oxygen quenches it, presumably leading to the production of $O_2^{\bullet-}$ (Eq 1):

$$AQ^{\bullet-} + O_2 \rightarrow AQ + O_2^{\bullet-} \quad (1)$$

Consistent with the above observations, ^{3}AQ was observed to decay with a similar lifetime, 5 μs, in argon-saturated solutions and it also disappeared when oxygen was allowed into the system. Weak transients could be observed in PBS living approximately 1 μs, however oxygen had no effect on their decay kinetics, neither was there any difference when was observed at 550 or 675 nm. They are thus tentatively attributed to aggregate species. A weak transient living 1.7 μs could be observed for $AQ^{\bullet-}$ (550 nm) in air-saturated planktonic yeast suspensions, whereas no signal was detectable at 675 nm (^{3}AQ) (Fig 6B). In the case of biofilms, $AQ^{\bullet-}$ could be detected only when the cells were incubated for 3 h (Fig 7). The lifetime of the transient was 170 μs in air-saturated samples. No evidence for the presence of ^{3}AQ in biofilms could be derived from transient absorption measurements (Fig 6).

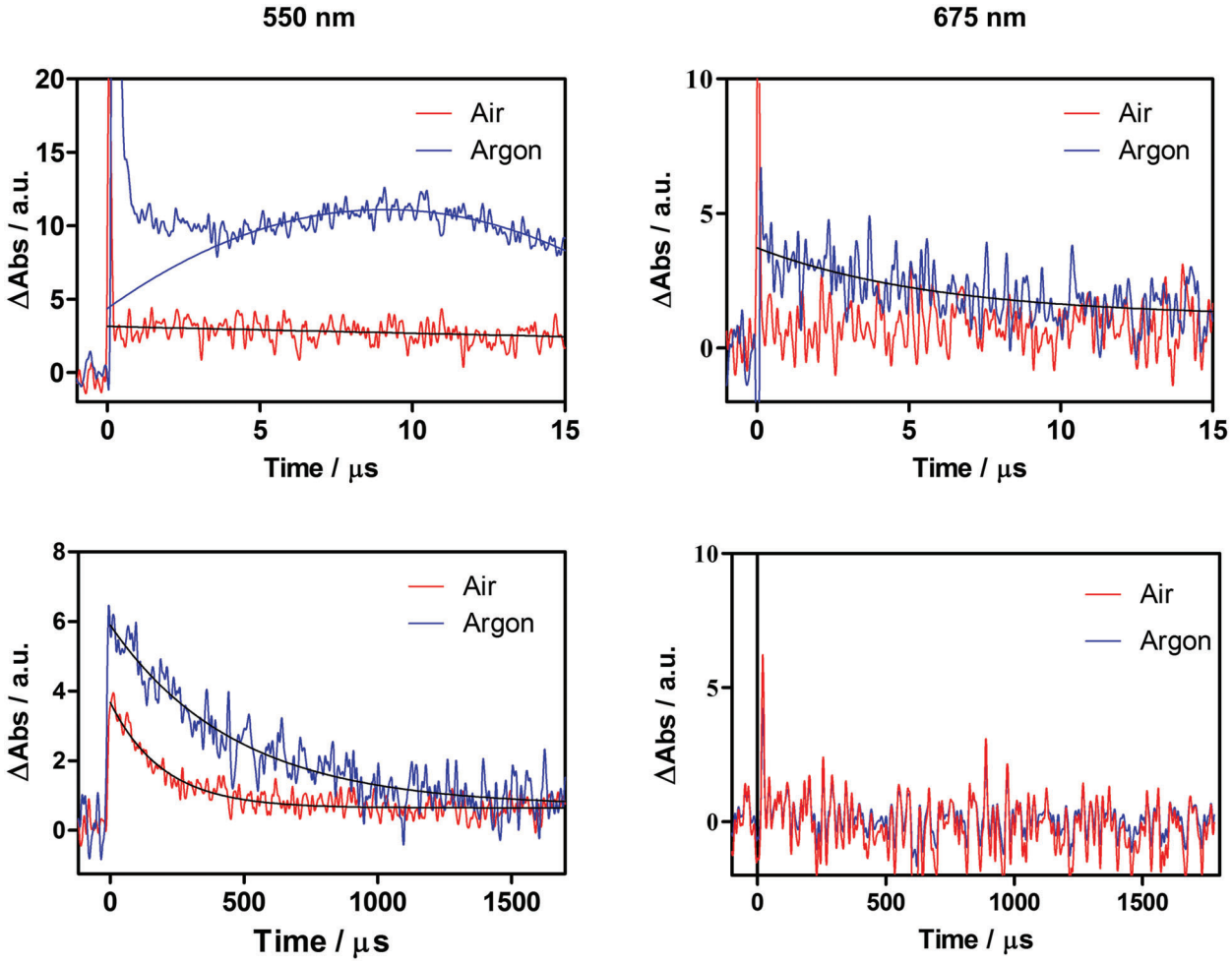

Fig 5. Transient absorption of 2 in argon- and air saturated- Cl_3CH solutions. Signals recorded at 550 nm correspond to $AQ^{\bullet-}$, whereas signal at 675 nm correspond to ^3AQ.

https://doi.org/10.1371/journal.pone.0181517.g005

Singlet oxygen measurements

Time-resolved near-IR luminescence detection is a powerful tool to study the process of $^1O_2$ photosensitization, since this ROS can be directly monitored through its phosphorescence at 1275 nm [26, 33–35]. Clear signals could be observed for **1** and **2** in $CHCl_3$ and PBS. The Φ_Δ values in $CHCl_3$ (0.34 and $<10^{-3}$ for **1** and **2**, respectively) were already reported by Núñez Montoya et al. [15,16]. In PBS, they were $\Phi_\Delta < 0.01$ for **1** and $\Phi_\Delta = 0.02$ for **2**.

Luminescence signals could also be recorded in biofilms (Fig 8) and were assigned to $^1O_2$ based on the spectral distribution (disappearance of the signal at 1325 nm, where $^1O_2$ shows almost no phosphorescence), and on the lengthening of the decay lifetime upon solvent deuteration [34]. Observation of $^1O_2$ indicates that ^3AQ is indeed formed, even if the concentration is too small to produce a transient absorption signal. By comparing the intensity of the phosphorescence signals for the two AQs, it is apparent that **2** generates approximately three-fold more $^1O_2$ than **1** in biofilms (Fig 8B). $^1O_2$ production was not detected when the biofilm was incubated in PBS with either AQ (Fig 8A).

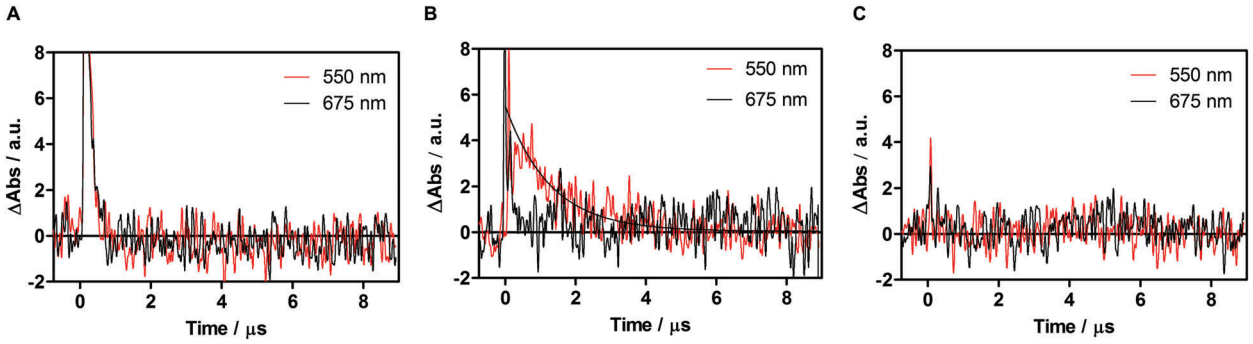

Fig 6. Transient absorption of air saturated- planktonic yeast suspension with 1 (A), 2 (B) and alone (C). Signals recorded at 550 nm correspond to $AQ^{\bullet-}$, whereas signal at 675 nm correspond to ^3AQ.

https://doi.org/10.1371/journal.pone.0181517.g006

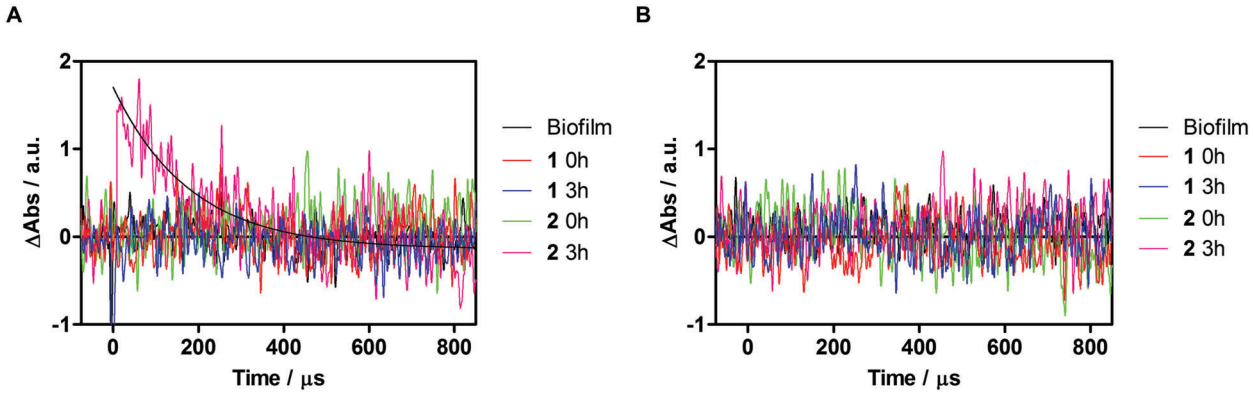

Fig 7. Transient absorption of air saturated- *C. tropicalis* biofilms with 1, 2 and alone at t = 0 and 3 hours of incubation. Signals recorded at 550 nm correspond to $AQ^{\bullet-}$(**A**), whereas signal at 675 nm correspond to ^3AQ (**B**).

https://doi.org/10.1371/journal.pone.0181517.g007

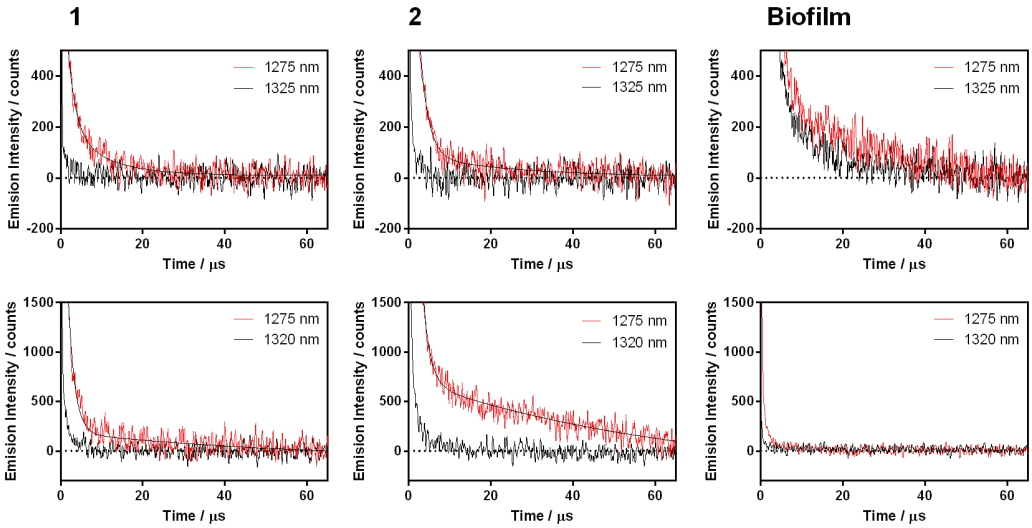

Fig 8. $^1O_2$ kinetics of 1 and 2 in *C. tropicalis* biofilm observed at 1275 nm and at 1325 nm (negative control) in PBS (A) and in biofilms incubated with D-PBS (B).

https://doi.org/10.1371/journal.pone.0181517.g008

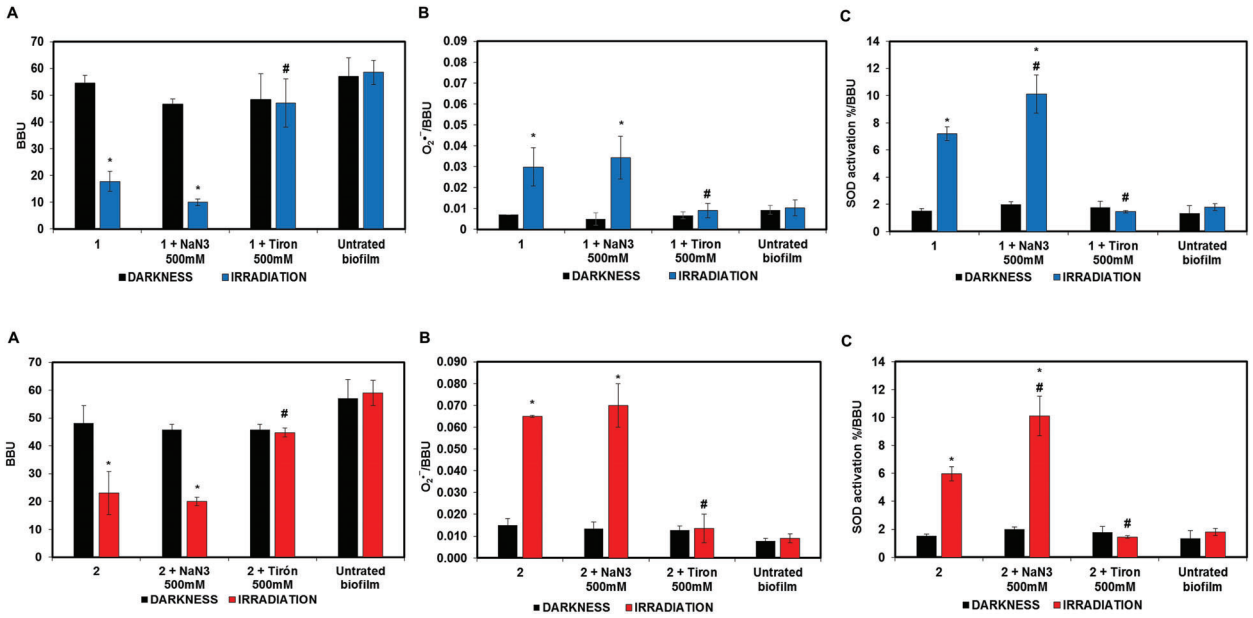

Fig 9. (A) Photo-induced *C. tropicalis* biofilm reduction by the AQs 1 and 2 in the presence of the specific ROS quenchers sodium azide and Tiron. (B) Superoxide radical production in *C. tropicalis* by AQ alone and in the presence of quenchers. (C) SOD activation in *C. tropicalis biofilms* by AQ alone and in the presence of quenchers. * $p < 0.05$ respect to biofilm # $p < 0.05$ AQ *vs* AQ + Quencher.

https://doi.org/10.1371/journal.pone.0181517.g009

Effect of ROS quenchers on the photo-induced biofilm reduction

The photo-induced biofilm reduction studies were repeated in the presence of specific ROS quenchers such as Tiron (for $O_2^{\bullet-}$) and sodium azide (for $^1O_2$). The photoinduced antibiofilm activity of **1** and **2** was not modified by sodium azide, whereas it was fully reversed by Tiron, reaching the control levels (biofilm) (Fig 9A). This implies that photostimulated AQs generate $O_2^{\bullet-}$, however quenching by Tiron scavenges their antifungal activity. This was corroborated by the NBT assay (Fig 9B), which demonstrated that the anti-biofilm activity enhancement under irradiation correlates with increased levels of $O_2^{\bullet-}$ and therefore with the enhanced activation of SOD (Fig 9C). Only in the presence of Tiron the production of $O_2^{\bullet-}$ and the activation of SOD return to their basal levels (biofilm).

Discussion

PDT of deeply-seated lesions uses red light owing to its higher penetration in tissues, however blue light is actually preferred for the treatment of surface infections and biofilms [36–39], which would be feasible with the current AQs. It is known that 410 nm blue light is capable of inactivating planktonic *Candida* spp. cells [40]. However, Fig 9A shows that the biomass of biofilms exposed to light without the AQs is not different from those with no drug and kept in the dark. The discrepancy is due the underlying reason may be that the light fluence used in that Zhang *et al*. study on planktonic cells [40], which was more than one order of magnitude larger than in the present work. While the AQs showed a similar antibiofilm effect under irradiation at the assayed concentration (56 μM ≈ 15 μg/mL), **2** was less cytotoxic than **1** on mammalian eukaryotic cells [24]. Specifically, **2** exhibited a CC_{50} value of 34.4 ± 0.2 μg/mL, whereas the CC_{50} value of 1 was 14.9 ± 0.2 μg/mL. It must be noted however that **1** showed a comparable antibiofilm activity already at 1.96 μg/mL.

Although the concentration of **1** was increased by one order of magnitude relative to that used in our previous publication [14], the activity on biofilms did not change appreciably. Specifically, a 63.5 ± 4.5% reduction was observed previously at 1.96 μg/mL (Table 1 in S1 File), whereas the currently observed decrease is 68.2 ± 6.7% at now at 14.22 μg/mL (56 μM) ($p > 0.05$). Thus, the antibiofilm effect of **1** does not change in this concentration range, which could be due to aggregation of **1** as indicated by the absorption spectra (Fig 4). The antibiofilm effect of **2** was similar to that previously observed, not surprisingly, because the concentration used was very similar.

The mechanism of photo-induced *C. tropicalis* biofilm reduction by two natural AQs, rubiadin and rubiadin-1-methyl ether, was studied as a means to identify the ROS involved in this photoprocess.

Absorption spectra (Fig 3) revealed the presence of AQ aggregates in PBS, planktonic yeast and biofilms, as indicated by the broadening of the bands and the changes in their relative intensity as compared to $CHCl_3$ [41,42]. Nevertheless, the situation observed in biofilms suggests an intermediate behaviour in which partial disaggregation occurs upon biofilm uptake.

In one hand, although it was not possible to detect triplet state absorption for any of the AQs in biofilms, observation of $^1O_2$ phosphorescence indicates that this species is actually formed. Once again, **2** shows a higher efficiency than **1**. There are no literature reports of the lifetime of $^1O_2$ in *C. tropicalis* biofilms, therefore it is not possible to confirm whether the decays are characteristic or not. Thus, we had to rely on the accepted tests for $^1O_2$ to ascertain the origin of the luminescence: spectral dependence on the phosphorescence intensity (higher at 1275 nm than at 1325 nm) and longer lifetime upon solvent deuteration. Biofilms incubated with **1** or **2** showed this pattern, more easily distinguishable in d-PBS incubated biofilms, confirming the assignment of the luminescence to $^1O_2$ phosphorescence. There is also a strong component that dominates the early part of the decay, which is due to laser light scattering and is unavoidable in non-transparent samples. Nevertheless, the contribution of $^1O_2$ to biofilm reduction must be negligible since sodium azide, a specific $^1O_2$ quencher, was not able to prevent it.

Fig 9B shows that biofilms generate a non-zero level of $O_2^{\bullet-}$ in the absence of light or AQ. The observation that incubation with AQs and exposure to light induced higher levels of $O_2^{\bullet-}$ 48 h after the treatment (Fig 9B) indicates that the intrinsic ability of the cell to produce $O_2^{\bullet-}$ had been perturbed. Since sodium azide did not quench the delayed production of $O_2^{\bullet-}$ but Tiron did, it can be concluded that "prompt" $O_2^{\bullet-}$ produced by photosensitization, but not $^1O_2$, is the main responsible for the perturbation of the oxidative balance of the cell that leads to an increase in the "delayed" production of $O_2^{\bullet-}$.

Tiron can react with both hydroxyl radicals ($OH^{\bullet}$) and $O_2^{\bullet-}$ [43]. However, since Tiron was added before irradiation and $OH^{\bullet}$ is a secondary product of $O_2^{\bullet-}$, Tiron would have prevented the formation of $OH^{\bullet}$ by scavenging its precursor, $O_2^{\bullet-}$. On the other hand, the radical anion of AQ **2**, which is a precursor of $O_2^{\bullet-}$ according to the reaction (1), was detected by transient absorption spectroscopy. Finally, $^1O_2$ cannot be a precursor of $O_2^{\bullet-}$, since azide, a well-known $^1O_2$ quencher, did not prevent its production nor the growth of the biofilms.

In summary, the observation that Tiron inhibits the photo-induced *C. tropicalis* biofilm reduction by the AQs (Fig 9A) suggests that production of $O_2^{\bullet-}$ by electron transfer quenching of the AQs excited states is the main component in the photosentizing mechanism.

Conclusions

The results above indicate that the biomass reduction of *C. tropicalis* biofilms produced by the assayed natural AQs, Rubiadin and Rubiadin-1-methyl ether, was mediated mainly by $O_2^{\bullet-}$

generation after exposure to light (Type-I photodynamic mechanism). Production of $^1O_2$ was observed in biofilm incubated with deuterated PBS, however its participation in the photo-induced biofilm reduction seems negligible.

Supporting information

S1 File. Marioni et al 2016-AQs biofilms. AQs reduce *Candida tropicalis* biofilms.
(PDF)

Acknowledgments

J. Marioni is a research fellow of CONICET. L.R. Comini, M.G. Paraje, J.L. Cabrera and S.C. Núnez Montoya are members of the Research Career of CONICET. R.B.-O. thanks the European Social Funds and the SUR del DEC de la Generalitat de Catalunya for his predoctoral fellowship (2016 FI_B1 00021).

Author Contributions

Conceptualization: Santi Nonell, Susana C. Núñez Montoya.

Formal analysis: Juliana Marioni, Roger Bresolí-Obach.

Funding acquisition: José L. Cabrera, Santi Nonell, Susana C. Núñez Montoya.

Investigation: Juliana Marioni, Roger Bresolí-Obach, Montserrat Agut, Laura R. Comini.

Methodology: Juliana Marioni, Roger Bresolí-Obach, Montserrat Agut, María G. Paraje, Santi Nonell, Susana C. Núñez Montoya.

Project administration: Santi Nonell, Susana C. Núñez Montoya.

Resources: Montserrat Agut, José L. Cabrera, María G. Paraje, Santi Nonell, Susana C. Núñez Montoya.

Supervision: Roger Bresolí-Obach, María G. Paraje, Santi Nonell, Susana C. Núñez Montoya.

Validation: María G. Paraje, Santi Nonell, Susana C. Núñez Montoya.

Visualization: Juliana Marioni, Roger Bresolí-Obach, Santi Nonell, Susana C. Núñez Montoya.

Writing – original draft: Juliana Marioni, Roger Bresolí-Obach, María G. Paraje, Santi Nonell, Susana C. Núñez Montoya.

Writing – review & editing: Juliana Marioni, Roger Bresolí-Obach, Santi Nonell, Susana C. Núñez Montoya.

References

1. Pereira Gonzalez F, Maich T. Photodynamic inactivation for controlling *Candida albicans* infections. Fungal Biology. 2011; 116(1): 1–10. https://doi.org/10.1016/j.funbio.2011.10.001 PMID: 22208597
2. Calzavara-Pinton P, Rossi MT, Sala R, Venturini M. Photodynamic antifungal chemotherapy. Photochem Photobiol. 2012; 88(3): 512–522. https://doi.org/10.1111/j.1751-1097.2012.01107.x PMID: 22313493
3. Rajendran M. Review Quinones as photosensitizer for photodynamic therapy: ROS generation, mechanism and detection methods. Photodiagnosis Photodyn Ther. 2016; 13: 175–187. https://doi.org/10.1016/j.pdpdt.2015.07.177 PMID: 26241780
4. Silva S, Negri M, Henriques M, Oliveira R, Williams DW, Azeredo J. *Candida glabrata*, *Candida parapsilosis* and *Candida tropicalis*: biology, epidemiology, pathogenicity and antifungal resistance. FEMS

Microbiol Rev. 2012; 36(2): 288–305. https://doi.org/10.1111/j.1574-6976.2011.00278.x PMID: 21569057

5. Khan MSA, Ahmad I, Aqil F, Owais M, Shahid M and Musarrat J. "Virulence and Pathogenicity of Fungal Pathogens with Special Reference to *C. albicans*," In: Ahmad I, Owais M, Shahid M and Aqil F, Eds., Combating Fungal Infections: Problems and Remedy, Springer- Verlag, Berlin, 2010. pp. 21–45.
6. Ramage G, Ranjith R, Leighann S, Craig W. Fungal Biofilm Resistance. Int J Microbiol. Article ID 528521, 14 pages, 2012.
7. Bizerra FC, Vataru Nakamura C, Poersch C, Estivalet Svidzinski TI, Borsato Quesada RM, Goldenberg S, et al. Characteristics of biofilm formation by *Candida tropicalis* and antifungal resistance. FEMS Yeast Res. 2008; 8(3): 442–450. https://doi.org/10.1111/j.1567-1364.2007.00347.x PMID: 18248413
8. Goldani LZ and Mário PSS. *Candida tropicalis* funguemia in a tertiary care hospital. J Infection. 2003; 46(3): 155–160.
9. Nucci M, Queiroz-Telles F, Tobón AM, Restrepo A, Colombo AL. Epidemiology of opportunistic fungal infections in Latin America. Clin Infect Dis. 2010; 51(5), 561–570. https://doi.org/10.1086/655683 PMID: 20658942
10. Núñez Montoya SC, Agnese AM, Pérez C, Tiraboschi IN, Cabrera JL. Pharmacological and toxicological activity of *Heterophyllaea pustulata* anthraquinone extracts. Phytomedicine. 2003; 10(6–7): 569–574. PMID: 13678245
11. Núñez Montoya SC, Agnese AM, Cabrera JL. Anthraquinones derivatives from *Heterophyllaea pustulata*. J Nat Prod. 2006; 69(5): 801–803. https://doi.org/10.1021/np050181o PMID: 16724844
12. Bacigalupo NM. 1993. Rubiaceae. In: Cabrera AL, ed. *Flora de la Provincia de Jujuy*. INTA: Buenos Aires, 375–80.
13. Marioni J, Arce JE, Cabrera JL, Paraje M G, Núñez Montoya SC. Reduction of *Candida tropicalis* biofilm by photoactivation of a *Heterophyllaea pustulata* extract. Pharm Biol. 2016; 54(12): 2791–2801. https://doi.org/10.1080/13880209.2016.1183683 PMID: 27256704
14. Marioni J, Da Silva MA, Cabrera JL, Núñez Montoya SC, Paraje MG. The anthraquinones rubiadin and its 1-methyl ether isolated from *Heterophyllaea pustulata* reduces *Candida tropicalis* biofilms formation. Phytomedicine. 2016; 23(12): 1321–1328. http://dx.doi.org/10.1016/j.phymed.2016.07.008 PMID: 27765351
15. Núñez Montoya SC, Comini LR, Sarmiento M, Becerra C, Albesa I, Argüello GA, et al. Natural anthraquinones probed as Type I and Type II photosensitizers: singlet oxygen and superoxide anion production. J Photochem Photobiol B. 2005; 78(1): 77–83. https://doi.org/10.1016/j.jphotobiol.2004.09.009 PMID: 15629252
16. Comini LR, Núñez Montoya SC, Sarmiento M, Cabrera JL, Argüello Gustavo A. Characterizing some photophysical, photochemical and photobiological properties of photosensitizing anthraquinones. J Photochem Photobiol A Chem. 2007; 188(2): 185–191. http://dx.doi.org/10.1016/j.jphotochem.2006.12.011
17. Clinical and Laboratory Standards Institute (CLSI). Reference Method for Broth Dilution Antifungal Susceptibility Testing of Yeasts; Approved Standard–Second Edition. CLSI document M27-A2 (ISBN1-56238-469-4). Clinical and Laboratory Standards Institute, 950 West Valley Road, Suite 2500, Wayne, Pennsylvania 19087 USA, 2002.
18. Price M, Reiners JJ, Santiago AM, Kessel D. Monitoring singlet oxygen and hydroxyl radical formation with fluorescent probes during photodynamic therapy. Photochem Photobiol. 2009; 85(5): 1177–1181. https://doi.org/10.1111/j.1751-1097.2009.00555.x PMID: 19508643
19. Kahler CP. Evaluation of the use of the solvent dimethyl sulfoxide in chemiluminescent studies. Blood Cells Mol Dis. 2000; 26(6): 626–633. https://doi.org/10.1006/bcmd.2000.0340 PMID: 11358355
20. Peralta MA, da Silva MA, Ortega MG, Cabrera JL, Paraje MG. Antifungal activity of a prenylated flavonoid from *Dalea elegans* against *Candida albicans* biofilms. Phytomedicine. 2015; 22(11): 975–80. http://dx.doi.org/10.1016/j.phymed.2015.07.003 PMID: 26407939
21. O´Toole GA, Kolter R. Initiation of biofilms formation in WCS365 proceeds via multiple, convergent signaling pathways a genetic analysis. Mol Microbiol. 1998; 28(3): 449–461.
22. Pierce CG, Uppuluri P, Tristan AR., Wormley FL Jr., Mowat E, Ramage G, et al. A simple and reproducible 96-well plate-based method for the formation of fungal biofilms and its application to antifungal susceptibility testing. Nat Protoc. 2008; 3(9): 1494–500. https://doi.org/10.1038/nport.2008.141 PMID: 18772877
23. COMSTAT. Technical University of Denmark, Kongens Lyngby, Dinamarca. http://www.comstat.dk. Last access in March 2016.

24. Konigheim BS, Comini LR, Grasso S, Aguilar JJ, Marioni J, Contigiani MS, et al. Determination of non-toxic and subtoxic concentrations of potential antiviral natural anthraquinones. Lat Am J of Pharm. 2012; 31(1): 51–56.
25. Comini LR, Núñez Montoya SC,. Argüello Gustavo A, Cabrera JL. Determinación del coeficiente de partición (log P) para derivados antraquinónicos aislados de *Heterophyllaea pustulata* Hook. f.(Rubiáceas). Acta Farmacéutica Bonaerense, 2006; 25(2): 252–255.
26. Jimenez-Banzo A, Ragàs X, Kapusta P, Nonell S. Time-resolved methods in biophysics. 7. Photon counting vs. analog time-resolved singlet oxygen phosphorescence detection. Photochem Photobiol Sci. 2008; 7(9): 1003–1010. https://doi.org/10.1039/b804333g PMID: 18754045
27. Schmidt RC, Dunsbach R, Wolff C. Phenalenone, a universal reference compound for the determination of quantum yields of singlet oxygen $O_2(^1\Delta_g)$ sensitization. J Photochem Photobiol A Chem. 1994; 79(1): 11–17. https://doi.org/10.1016/1010-6030(93)03746-4
28. Martí C, Jürgens O, Cuenca O, Casals M Nonell S. Aromatic ketones as standards for singlet molecular oxygen $O_2(^1\Delta_g)$ photosensitization. Time-resolved photoacoustic and NIR emission studies. J Photochem Photobiol A Chem, 1996; 97(1–2): 11–18. https://doi.org/10.1016/1010-6030(96)04321-3
29. Shida T. "Electronic absorption spectra of radical ions", Physical Sciences Data 34, 1988, Elsevier, Amsterdam.
30. Berry D, Mader E,. Lee TK, Woebken D, Wang Y, Zhu D, et al. Tracking heavy water (D_2O) incorporation for identifying and sorting active microbial cells. Proc Natl Acad Sci USA. 2015; 112(2): E194–E203. https://doi.org/10.1073/pnas.1420406112 PMID: 25550518
31. Paz-Cristobal M, Royo D, Rezusta A, Andres-Ciriano E, Alejandre MC, Meis JF, et al. Photodynamic fungicidal efficacy of hypericin and dimethyl methylene blue against azole-resistant *Candida albicans* strains. Mycoses. 2014; 57(1): 35–42. https://doi.org/10.1111/myc.12099 PMID: 23905682
32. Angel Villegas N, Baronetti JL, Albesa I, Etcheverría A. Becerra MC, Padola NL, et al. Effect of antibiotics on cellular stress generated in *Shiga toxin*-producing *Escherichia coli* O157: H7 and non-O157 biofilms. Toxicol In Vitro. 2015; 29(7): 1692–700. http://dx.doi.org/10.1016/j.tiv.2015.06.025 PMID: 26130220
33. López-Chicón P, Paz-Cristobal MP, Rezusta A, Aspiroz C, Royo Cañas M, Andres- Ciriano E, et al. On the mechanism of *Candida spp* photoinactivation by hypericin. Photochem Photobiol Sci. 2012; 11(6); 1099–107. https://doi.org/10.1039/c2pp25105a PMID: 22566080
34. Snyder JW, Skovsen E, Lambert JDC, Poulsen L., Ogilby PR. Optical detection of singlet oxygen from single cells. Phys Chem Chem Phys. 2006; 8(37): 4280–4293. https://doi.org/10.1039/b609070m PMID: 16986070
35. Ragàs X, Agut M, Nonell S. Singlet oxygen in *Escherichia coli*: New insights for antimicrobial photodynamic therapy. Free Radic Biol Med. 2010; 49(5): 770–776. https://doi.org/10.1016/j.freeradbiomed.2010.05.027 PMID: 20638940
36. Dijkstra AT, Majoie IML, Van Dongen JWF, Van Weelden H, Van Vloten WA. Photodynamic therapy with violet light and topical δ-aminolaevulinic acid in the treatment of actinic keratosis, Bowen's disease and basal cell carcinoma. J Eur Acad Dermatol Venereol 2001; 15(6); 550–554. PMID: 11843215
37. Allevato MA. Terapia fotodinámica. Act Terap Dermatol. 2006; 29: 302–312.
38. Davids LM, Kleemann B, Kacerovská D, Pizinger K, Kidson SH. Hypericin phototoxicity induces different modes of cell death in melanoma and human skin cells. J Photochem Photobiol B. 2008; 91(2); 67–76.
39. Cieplik F, Tabenski L, Buchalla W, Maisch T. Antimicrobial photodynamic therapy for inactivation of biofilms formed by oral key pathogens. Front microbiol. 2014; 5: 405. https://doi.org/10.3389/fmicb.2014.00405 PMID: 25161649
40. Zhang Y, Zhu Y, Chen J, Wang Y, Sherwood ME, Murray CK, et al. Antimicrobial blue light inactivation of *Candida albicans*: in vitro and in vivo studies. Virulence. 2016; 7(5):536–45. https://doi.org/10.1080/21505594.2016.1155015 PMID: 26909654
41. Eisfeld A. & Briggs JS. The J-and H-bands of organic dye aggregates. Chem Phys. 2006; 324(2): 376–384. http://dx.doi.org/10.1016/j.chemphys.2005.11.015
42. Gouloumis A, González-Rodríguez D, Vázquez P, Torres T, Liu S, Echegoyen L, et al. Control over charge separation in phthalocyanine-anthraquinone conjugates as a function of the aggregation status. J Am Chem Soc. 2006; 128(39); 12674–12684. https://doi.org/10.1021/ja055344+ PMID: 17002361
43. Bors W, Saran M, Michel C. Pulse-radiolytic investigations of catechols and catecholamines II. Reactions of Tiron with oxygen radical species. Biochim Biophys Acta.1979; 582(3): 537–542. https://doi.org/10.1016/0304-4165(79)90145-4 PMID: 217444